DEVELOPMENT OF CDK2 INHIBITORS TO OVERCOME PRIMARY AND ACQUIRED RESISTANCE TO CDK4/6 INHIBITION

CLAIRE R. HALL[1], ANGELA L. RAUER[1], KERRY A. DILLON[1], ANNE Y. LAI[1], JULIE E. PICKETT[2], WILLIAM J. ZUERCHER[2], CARROW I. WELLS[2], JOHN E. BISI[1], JAY C. STRUM[1]

[1]G1 THERAPEUTICS, INC., RESEARCH TRIANGLE PARK, NC, USA; [2]STRUCTURAL GENOMICS CONSORTIUM, DIVISION OF CHEMICAL BIOLOGY AND MEDICINAL CHEMISTRY, UNC ESHELMAN SCHOOL OF PHARMACY, UNIVERSITY OF NORTH CAROLINA AT CHAPEL HILL, CHAPEL HILL, NC, USA

INTRODUCTION

The cyclin-dependent kinase (CDK) family of proteins is associated with cell cycle progression and transcriptional regulation. Recent advances in treatments using CDK inhibition have focused on targeting cyclin-dependent kinases 4 and 6 (CDK4/6), with regulatory approvals of palbociclib, ribociclib and abemaciclib, and ongoing clinical development of lerociclib. Although CDK4/6 inhibitors are part of established treatment regimens for certain forms of breast cancer (BC), insensitivity to CDK4/6 inhibition has been found in primary resistance, such as forms of triple negative breast cancers (TNBC), or acquired resistance, by prior treatment with a CDK4/6 inhibitor in ER+ Her2- breast cancer. Overexpression of cyclin E has been described in tumors insensitive to CDK4/6 inhibitors as well as in ovarian and lung tumor types. Cyclin-dependent kinase 2 (CDK2) complexes with cyclin E playing a role in the phosphorylation of Rb and the G1 to S-phase transition of the cell cycle, as well as in assembly of the pre-replication complex in S. CDK2 also binds cyclin A, forming a complex that is required to initiate DNA synthesis in S and activate CDK1/CyclinB for the G2-M transition. Inhibition of CDK2 gives another promising option of using CDK inhibitors to alter cell cycle progression in tumors. We are focused on developing a novel, potent, and selective inhibitor of CDK2 to treat patients whose tumors are insensitive to CDK4/6 inhibition, either by primary resistance or acquired resistance by prior treatment with a CDK4/6 inhibitor. Utilizing medicinal chemistry and structure activity relationship (SAR) modeling, starting from our proprietary scaffold, a series of small molecule CDK2 inhibitors with drug-like properties was generated. We have identified molecules with sub-nanomolar biochemical IC_{50} values for CDK2 when complexed with cyclin A and cyclin E. Here we present the potent and dose-dependent activity of these compounds in multiple settings *in vitro* evaluating the effects of CDK2 inhibition.

RESULTS

FIGURE 1. DEVELOPMENT OF SMALL MOLECULE INHIBITORS POTENT AGAINST CDK2/CYCLINE

A.

Inhibitor	Biochemical IC_{50} (nM)								
	CDK1/ CyclinB1	CDK2/ CyclinA	CDK2/ CyclinE	CDK3/ CyclinE	CDK4/ CyclinD1	CDK5/ p35	CDK6/ CyclinD3	CDK7/ CyclinH	CDK9/ CyclinT
CDK2i-1	1290	123	35	147	1	203	3	716	65
CDK2i-2	79	25	14	34	74	36	263	205	45
CDK2i-3	451	22	5	23	1	58	3	1980	1130
CDK2i-4	6	0.5	0.5	3	12	4	37	133	5
CDK2i-5	1	0.1	0.1	0.5	4	0.4	8	28	2
CDK2i-6	8	0.9	0.4	2	1	2	3	73	11
PF-06873600	2	0.3	0.3	2	2	0.3	4	47	43

B.

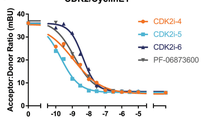

Inhibitor	IC_{50} (nM)
CDK2i-4	1
CDK2i-5	0.2
CDK2i-6	4
PF-06873600	2

(A) Biochemical profiles of novel and potent CDK2 inhibitors against a panel of CDKs and respective binding partners. Assays were completed in a 12 point dose-response format by Nanosyn, Inc. Results are shown as nanomolar IC_{50} concentrations against each target. CDK2 inhibitors 4, 5, and 6 have sub-nanomolar potencies against CDK2/CyclinE. Pfizer's CDK2 inhibitor, PF-06873600, was used as a reference compound. (B) NanoBRET Target Engagement Intracellular Kinase Assay results demonstrating potent binding of CDK2/CyclinE in cells by CDK2 inhibitors.

FIGURE 2. KINASE SELECTIVITY OF CDK2 INHIBITORS

A.

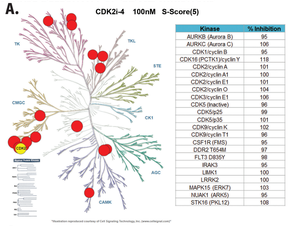

Kinase	% Inhibition
AURKB (Aurora B)	95
AURKC (Aurora C)	106
CDK1/cyclin B	95
CDK16 (PCTK1)/cyclin Y	118
CDK2/cyclin A	101
CDK2/cyclin A1	100
CDK2/cyclin E1	101
CDK2/cyclin O	104
CDK3/cyclin E1	106
CDK5 (inactive)	96
CDK5/p25	99
CDK5/p35	101
CDK9/cyclin K	102
CDK9/cyclin T1	96
CSF1R (FMS)	95
DDR2 T654M	97
FLT3 D835Y	98
IRAK3	95
LIMK1	100
LRRK2	100
MAPK15 (ERK7)	103
MUAK1 (ARK5)	96
STK16 (PKL12)	108

B.

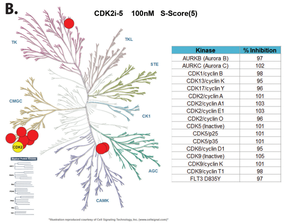

Kinase	% Inhibition
AURKB (Aurora B)	97
AURKC (Aurora C)	102
CDK1/cyclin B	98
CDK13/cyclin K	95
CDK17/cyclin Y	96
CDK2/cyclin A	101
CDK2/cyclin A1	103
CDK2/cyclin E1	103
CDK2/cyclin O	96
CDK5 (inactive)	101
CDK5/p25	101
CDK5/p35	101
CDK9/cyclin D1	95
CDK9 (inactive)	105
CDK9/cyclin K	101
CDK9/cyclin T1	96
FLT3 D835Y	97

C.

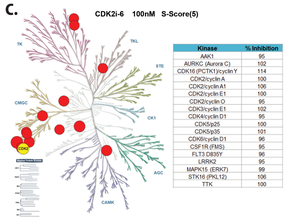

Kinase	% Inhibition
AAK1	95
AURKC (Aurora C)	102
CDK16 (PCTK1)/cyclin Y	114
CDK2/cyclin A	100
CDK2/cyclin A1	100
CDK2/cyclin E1	100
CDK2/cyclin O	95
CDK3/cyclin E1	102
CDK4/cyclin D1	95
CDK5/p25	100
CDK5/p35	101
CDK9/cyclin D1	96
CSF1R (FMS)	95
FLT3 D835Y	96
LRRK2	96
MAPK15 (ERK7)	99
STK16 (PKL12)	106
TTK	100

Kinome screens of three CDK2 inhibitors against a panel of 485 kinases. Screens performed by SelectScreen Kinase Profiling Services at Thermo Fisher Scientific. Portrayed are kinases inhibited over 95% on a kinome tree via Kinhub.org from Cell Signaling Technology, Inc. CDK2 is shown with a yellow circle. Corresponding tables list kinase or complex name and average % inhibition. (A) CDK2i-4 assessed at 200x the biochemical IC_{50} of CDK2/CyclinE. (B) CDK2i-5 assessed at 1000x the biochemical IC_{50} of CDK2/CyclinE. (C) CDK2i-6 assessed at 250x the biochemical IC_{50} of CDK2/CyclinE. All three inhibitors exhibit significant binding to the target protein.

RESULTS

FIGURE 3. GENERATION OF PALBOCICLIB-RESISTANT MCF7 CELLS

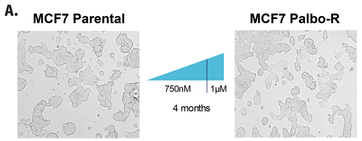

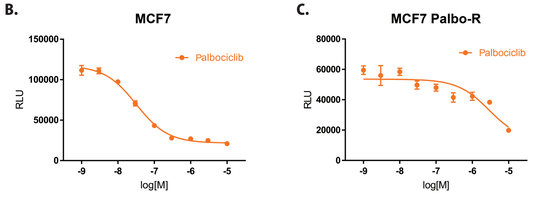

Cell Line	palbociclib IC_{50} (nM)
MCF7	33
MCF7 Palbo-R	2890

(A) MCF7 Parental cells (ATCC, ER+ Her2- BC, CDK4/6 dependent) were maintained in culture for four months in complete media (EMEM/ 10% FBS/ glutamax/ insulin) as control. MCF7 palbociclib-resistant (Palbo-R) cells were maintained in complete media plus palbociclib for three months at ~IC_{90} (750nM) followed by one month at 1µM. Pictures of the cells in culture depict the similar morphology and growth of the parental and resistant cell lines. 6-Day CellTiter Glo results for (B) MCF7 and (C) MCF7 Palbo-R cell lines treated with palbociclib from 1nM to 10µM, demonstrating an 87x increase of IC_{50} from MCF7 control cell line to Palbo-R cell line.

FIGURE 4. CHARACTERIZATION OF PALBOCICLIB-RESISTANT MCF7 CELLS

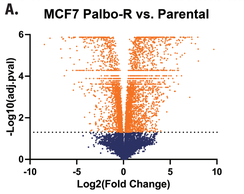

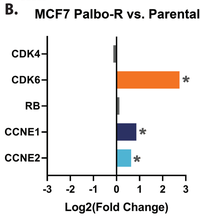

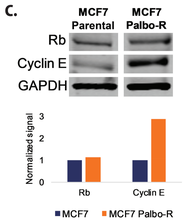

Whole transcriptome profiling was performed on MCF7 Parental and MCF7 Palbo-R cells by RNA-Seq. Libraries were prepared using the Illumina TruSeq Stranded mRNA assay and paired-end sequenced (2x50bp) on the Illumina HiSeq platform. (A) Pairwise comparison of transcript level in MCF7 Palbo-R vs. parental. 6039 genes out of 17383 detectable genes were differentially expressed (orange), with adjusted p-value <0.05. (B) Log2 fold change of genes of interest shown with * denoting statistical significance, adjusted p-value <0.05. (C) Western blot analysis of MCF7 Parental and MCF7 Palbo-R cells demonstrating an increase in the ratio of cyclin E levels in Palbo-R cells, with quantitation of normalized signal to loading control, GAPDH, located below.

FIGURE 5. CDK2 INHIBITORS PREVENT INCORPORATION OF EdU IN S-PHASE OF CELL CYCLE

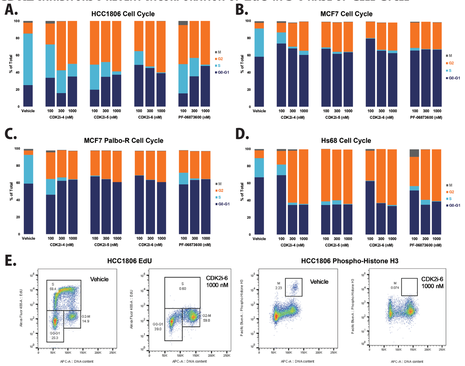

(A) HCC1806 (TNBC, CDK4/6 independent), (B) MCF7, (C) MCF7 Palbo-R, and (D) Hs68 (normal human fibroblast, CDK4/6 dependent) cell lines were treated with CDK2 inhibitors for 24 hours. Cell cycle profiles were evaluated following treatment via Flow Cytometry using FlowJo (v10.0) software. All four cell lines show a dose-dependent decrease in the incorporation of EdU during the S-phase of the cell cycle and a decrease in phosphorylated-histone H3 (Ser10). (E) Representative flow gating for FxCycle DNA stain, Click-iT™ EdU Flow Cytometry Assay Kit, and Phospho-Histone H3 conjugated antibody from HCC1806 samples treated with vehicle and CDK2i-6 at 1000nM.

FIGURE 6. CDK2 INHIBITORS DECREASE PHOSPHORYLATION OF Rb

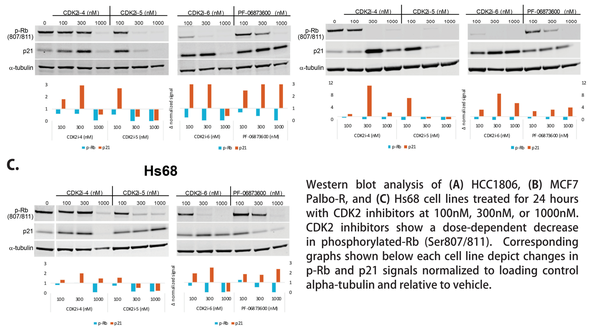

Western blot analysis of (A) HCC1806, (B) MCF7 Palbo-R, and (C) Hs68 cell lines treated for 24 hours with CDK2 inhibitors at 100nM, 300nM, or 1000nM. CDK2 inhibitors show a dose-dependent decrease in phosphorylated-Rb (Ser807/811). Corresponding graphs shown below each cell line depict changes in p-Rb and p21 signals normalized to loading control alpha-tubulin and relative to vehicle.

FIGURE 7. CDK2 INHIBITORS PREVENT PROLIFERATION OF TNBC, MCF7 PALBO-R, AND NORMAL CELLS

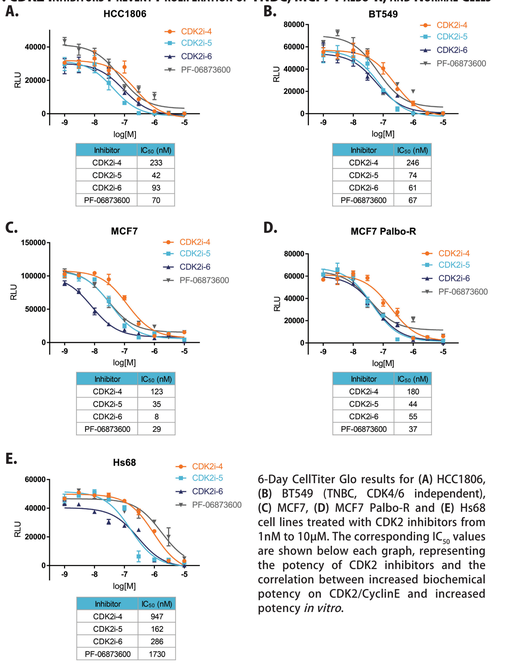

Inhibitor	IC_{50} (nM)
CDK2i-4	233
CDK2i-5	42
CDK2i-6	93
PF-06873600	70

Inhibitor	IC_{50} (nM)
CDK2i-4	246
CDK2i-5	74
CDK2i-6	61
PF-06873600	67

Inhibitor	IC_{50} (nM)
CDK2i-4	123
CDK2i-5	35
CDK2i-6	8
PF-06873600	29

Inhibitor	IC_{50} (nM)
CDK2i-4	180
CDK2i-5	44
CDK2i-6	55
PF-06873600	37

Inhibitor	IC_{50} (nM)
CDK2i-4	947
CDK2i-5	162
CDK2i-6	286
PF-06873600	1730

6-Day CellTiter Glo results for (A) HCC1806, (B) BT549 (TNBC, CDK4/6 independent), (C) MCF7, (D) MCF7 Palbo-R and (E) Hs68 cell lines treated with CDK2 inhibitors from 1nM to 10µM. The corresponding IC_{50} values are shown below each graph, representing the potency of CDK2 inhibitors and the correlation between increased biochemical potency on CDK2/CyclinE and increased potency *in vitro*.

FIGURE 8. CDK2 INHIBITORS DO NOT ELICIT CASPASE 3/7 ACTIVATION AT 24 HOURS

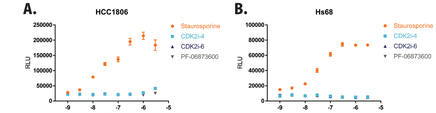

Caspase Glo 3/7 results for (A) HCC1806 and (B) Hs68 cell lines treated with CDK2 inhibitors and staurosporine control from 1 nM to 3 µM for 24 hours. The data demonstrates the clear activation of caspase 3/7 by staurosporine and no caspase 3/7 activation by CDK2 inhibitors.

SUMMARY

- Three novel small molecule inhibitors were identified with sub-nanomolar biochemical IC_{50} values against CDK2 when complexed with cyclin E or cyclin A.
- These CDK2 inhibitors were evaluated *in vitro* and shown to potently inhibit EdU incorporation and cell proliferation in TNBC and MCF7 Palbo-R cell lines.
- These potent CDK2 inhibitors demonstrate a potentially promising method of treating tumors with primary or acquired resistance to CDK4/6 inhibitors.
- Ongoing and future work for the lead CDK2 inhibitor includes PK studies and *in vivo* studies evaluating anti-tumor efficacy in mouse xenograft models.